

Investigating Large 2D Arrays for Photoacoustic and Acoustic Imaging using CMUT Technology

Srikant Vaithilingam*, Te-Jen Ma*, Yukio Furukawa*, Ömer Oralkan*, Aya Kamaya†, Kazutoshi Torashima*, Mario Kupnik*, Ira O. Wygant*, Xuefeng Zhuang*, R. Brooke Jeffrey Jr† and Butrus T. Khuri-Yakub*

*Edward L. Ginzton Laboratory, Stanford University, Stanford, CA 94305, USA

†Department of Radiology, Stanford University Medical Center, Stanford University, Stanford, CA 94305, USA

Abstract—In this paper, we investigate using a large aperture (64 x 64 element array) to perform photoacoustic and acoustic imaging by mechanically scanning a smaller array (16 x 16 elements) of capacitive micromachined ultrasonic transducers (CMUTs). We show results from the imaging of: 1) A fishing-line phantom. 2) Tubes embedded in chicken breast tissue containing the contrast agent indocyanine green (ICG), pig blood and a mixture of the two. The tubes were embedded at a depth of 0.8 cm inside the tissue and were at an overall distance of 1.9 cm from the CMUT array. Three-dimensional volume rendered images of traditional pulse-echo data as well as photoacoustic data are shown.

I. INTRODUCTION

Photoacoustic imaging (PAI), also called optoacoustic imaging, is a promising medical imaging technology because it combines the contrast information of optical imaging with the spatial resolution of acoustic imaging. It is a non-ionizing and non-invasive imaging modality. Functional imaging and molecular imaging are potential applications of PAI [1]. In this work, we use capacitive micromachined ultrasonic transducers (CMUTs) to perform both photoacoustic and acoustic imaging thereby providing mechanical and functional information respectively. Our final goal is to develop a complete, real-time three dimensional photoacoustic imaging system using large 2D CMUT arrays. As steps toward this goal, in this paper, we investigated imaging using a large aperture (64 x 64 element array) by mechanically scanning a 16 x 16 element CMUT array with integrated electronics. In particular, two phantoms were imaged. The first phantom was a fishing-line phantom. The second phantom consisted of tubes embedded in chicken breast tissue. The tubes contained pig blood, indocyanine green (ICG) dye and a mixture of both. This paper builds upon the work presented in an earlier conference paper [2].

II. METHODS

A. CMUT and integrated electronics

A 16 x 16 element CMUT array with integrated electronics was used to perform the experiments. Key parameters of this particular CMUT array are shown in Table I. The array was fabricated using a sacrificial layer etch process [3], [4]. The transducer array was flip-chip bonded to a custom-designed integrated circuit (IC) that comprises the front-end circuitry. Integrating the electronics in this manner mitigates the effect of parasitic cable capacitance and simplifies connecting the transducer array to an external signal processing system. The

IC provides a transmit and receive circuit to every element of the array. This circuit consists of a pulser, a transimpedance amplifier, and a switch that protects the low-voltage amplifier electronics from the pulser's output [5]. In this initial implementation, the IC only allowed a single element to transmit and receive at a time. Thus, with no averaging, 256 pulses were required to acquire a single image. A typical pulse-echo a-scan from an oil-air interface, 3.6 cm away from the array, is shown in Fig. 1. The center frequency of the array was measured to be 3.3 MHz. The input-referred pressure noise or noise equivalent pressure (NEP) for the device used in these experiments was measured to be $2.6 \text{ mPa}/\sqrt{\text{Hz}}$.

TABLE I
CMUT ARRAY PARAMETERS

Array size (elements)	16 x 16
Element pitch (μm)	250
CMUT membrane diameter (μm)	30
Number of membranes per element	36
Membrane thickness (μm)	0.5
Cavity thickness (μm)	0.1
Insulating layer thickness (μm)	0.15
Silicon substrate thickness (μm)	400
Flip-chip bond pad diameter (μm)	50
Through-wafer interconnect diameter (μm)	20
Silicon wafer resistivity ($\Omega\text{-cm}$)	>10,000

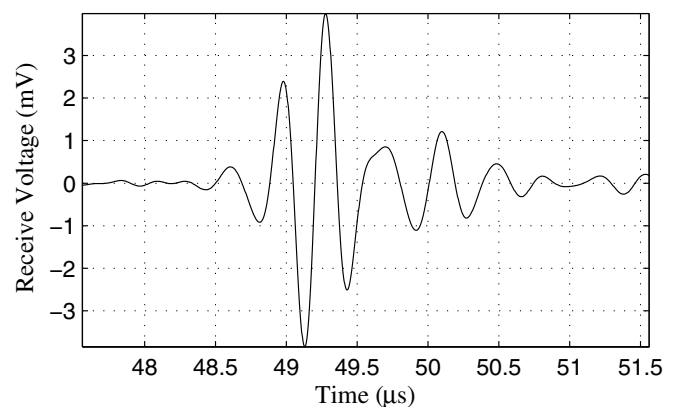


Fig. 1. Typical pulse-echo a-scan from a plane reflector 3.6 cm away from the transducer.

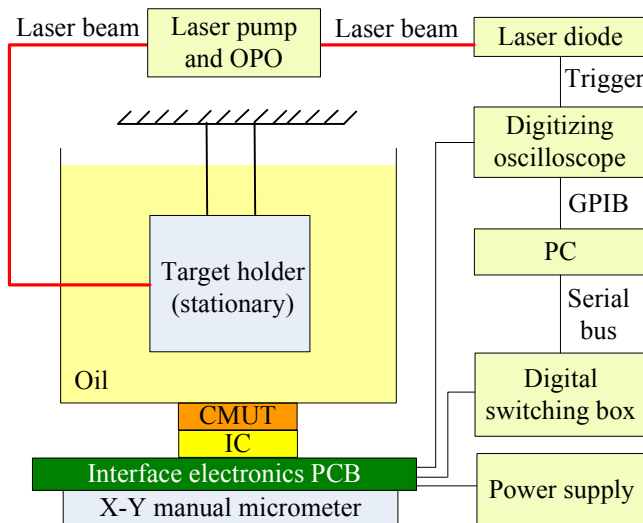


Fig. 2. Schematic of the experimental setup.

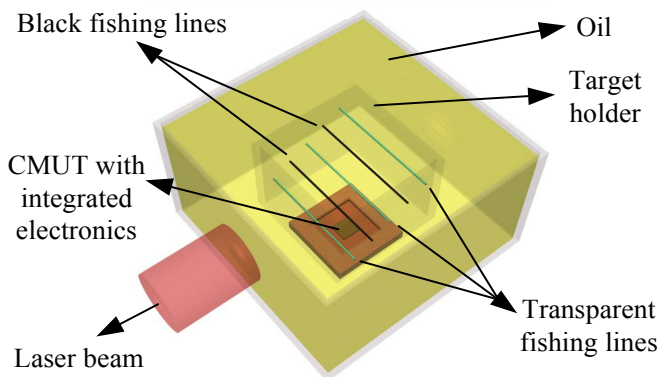


Fig. 3. Graphic of fishing line phantom in experimental setup.

B. Experimental Setup

For these experiments, the phantom to be imaged was suspended in an acrylic tank of size 12 cm x 12 cm x 7 cm (Fig. 2). A rectangular hole was cut at the bottom of the tank to create an acoustic window for the array. The tank was then glued to a ceramic package that contained the 16 x 16 element CMUT array flip-chip bonded to an IC. Vegetable oil was used to couple ultrasound between the CMUT array and phantom because it is nonconducting; thus, we could test the device in immersion without insulating the bond wires and electrodes of the device. We have previously demonstrated CMUTs insulated with parylene and PDMS for operation in water [6], [7].

The CMUT array and tank were mounted on a precision x-y translational stage to enable planar scanning and emulation of a 64 x 64 element CMUT array. The method employed was as follows: After one data set was acquired, the array was translated 4 mm (length of the array) along the x-direction and another data set was acquired. Further data sets were obtained by translating 4 mm along the y-direction as well. In this manner 16 total data sets were acquired. An image

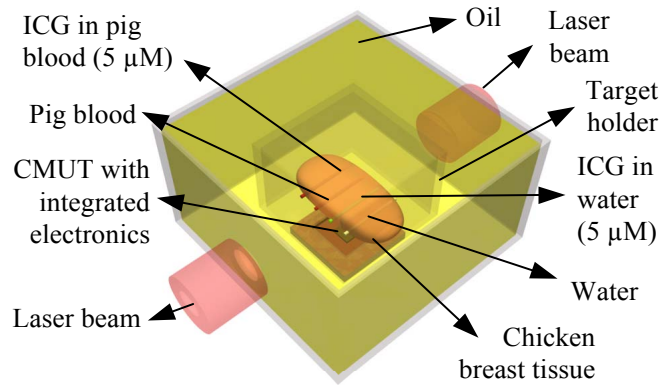


Fig. 4. Graphic of chicken breast phantom in experimental setup.

reconstructed from this data will be equivalent to that of an image reconstructed using a 64 x 64 element CMUT array. The phantom was illuminated from either one side or both sides of the tank (depending on the experiment) by a laser beam emitted from an optical parametric oscillator (OPO) pumped by a Q-switched Nd:YAG laser (Continuum SLIII-10). The laser pulses had a pulse-width of 5 ns and a repetition rate of 10 Hz. The laser beam was guided to the tank using free-space optics.

Two different phantoms were imaged. The first phantom was a resolution phantom consisting of three transparent 150 μm diameter fishing lines and two black 180 μm diameter fishing lines. The basic geometry of the phantom is shown in Fig. 3. We used single sided illumination for this phantom while gathering the photoacoustic data. The laser beam had a diameter of 2.5 cm, wavelength of 710 nm and a fluence of 5.23 mJ/cm^2 . The second phantom consisted of four polyethylene tubes embedded in chicken breast tissue. The inner diameter of the tubes was 1.19 mm and the outer diameter was 1.70 mm. The first tube was filled with de-ionized water; the second tube was filled with ICG solution in de-ionized water (5 μM); the third tube contained pig blood; the last tube was ICG mixed with pig blood (5 μM). For the chicken phantom, we used double-sided laser illumination as illustrated in Fig. 4. Each laser beam had a diameter of 1.5 cm and a fluence of 8.99 mJ/cm^2 and 13.69 mJ/cm^2 respectively. We used a laser wavelength of 775 nm to gather the photoacoustic data since the peak ICG absorption is at this wavelength for the concentrations used [8].

C. Image Reconstruction

The images were reconstructed using the classical synthetic aperture (SA) focusing technique (implemented by standard delay-and-sum beamforming) along with a coherence factor weighting [9], [10], [11]. The a-scan from each (x,y) position of the transducer was bandpass filtered and appropriately delayed and summed. Note that the coherence factor weighting is multiplied on a point-by-point basis with the image obtained from synthetic aperture focusing. Using this weighting reduces focusing errors resulting from sound velocity inhomogeneities.

The final photoacoustic and acoustic images were log compressed according to the dynamic range desired before being co-registered.

III. RESULTS AND DISCUSSION

Conventional pulse-echo imaging data and photoacoustic imaging data were acquired for both phantoms. Medical image viewing software [12] was used to render the acquired volumetric images.

A. Fishing line phantom

The pulse-echo data was averaged 32 times while the photoacoustic data was averaged 8 times. Volumetric images of the phantom, reconstructed using the 64 x 64 aperture data set, are shown in Fig. 5. In the pulse-echo image (Fig. 5a) all 5 fishing lines are seen since the color of the fishing lines is unimportant to the impinging pressure wave. However in the photoacoustic image (Fig. 5b) only the two black fishing lines are apparent since the transparent fishing lines do not absorb any light. The pulse-echo and photoacoustic images are co-registered and overlaid on each other as shown in Fig. 5c. In the pulse-echo image, the two black fishing lines are thicker than the transparent fishing lines which is in good agreement with the fact that the black fishing lines have a 180 μm diameter as opposed to the transparent fishing lines which have a 150 μm diameter. For comparison, the photoacoustic and pulse-echo images reconstructed using data from a 16 x 16 aperture is shown in Fig. 6. The image quality, field of view and resolution in Fig. 6 are much poorer than the image reconstructed using the 64 x 64 aperture.

B. Chicken breast phantom

The pulse-echo data was averaged 64 times while the photoacoustic data was averaged 8 times. Volumetric images of the phantom reconstructed using the 64 x 64 aperture data set are shown in Fig. 7. In the pulse-echo image (Fig. 7a) all the 4 embedded tubes can be seen. However in the photoacoustic image (Fig. 7b) only 3 tubes are visible. The tubes filled with ICG, blood and a mixture of the two can be seen while the tube filled with de-ionized water is not visible. This is expected as at the wavelength of laser light used, 775 nm, water has a low absorption coefficient. The pulse-echo and photoacoustic images are co-registered and overlaid on each other as shown in Fig. 5c. The tubes were embedded at a depth of 0.8 cm inside the tissue and were about 1.9 cm from the CMUT array surface.

IV. CONCLUSION

We have demonstrated true three-dimensional photoacoustic imaging using two-dimensional CMUT arrays with integrated electronics. Images from a fishing line phantom and chicken breast phantom are shown. We showed how the image quality dramatically improves when a large aperture is used to perform the imaging. ICG at a concentration of 5 μM and pig blood were detected against a background of chicken tissue. All these experimental results are promising for the

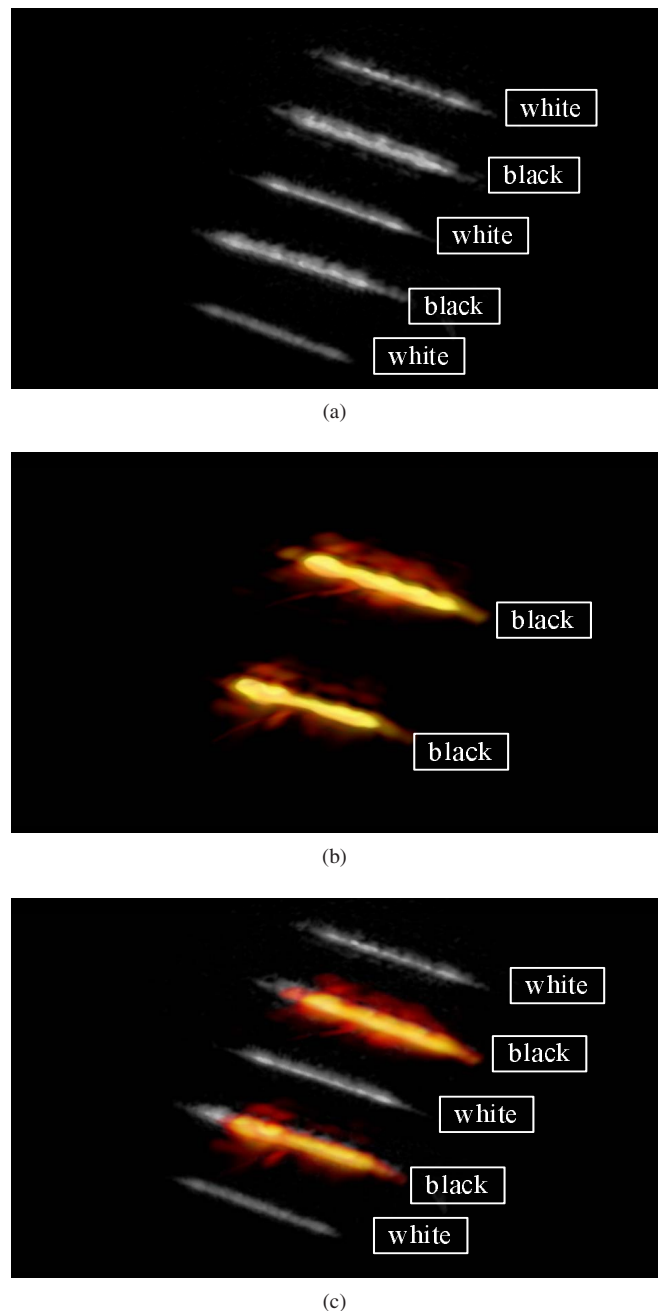


Fig. 5. Images of the fishing line phantom reconstructed using the data from a 64 x 64 aperture: (a) 3D rendered pulse-echo image (b) 3D rendered photoacoustic image (c) 3D rendered photoacoustic (red) image overlaid on pulse-echo image (gray-scale).

further development of CMUTs for photoacoustic imaging. This involves designing large CMUT arrays by leveraging the latest advances in MEMS fabrication technology, such as wafer bonding techniques. We are currently actively working on fabricating a true 64 x 64 element array as well as improving our electronic ICs to receive signals from more than one element at a time to facilitate real-time imaging.

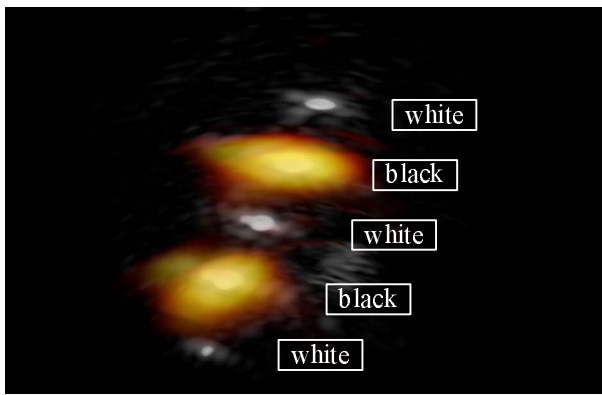


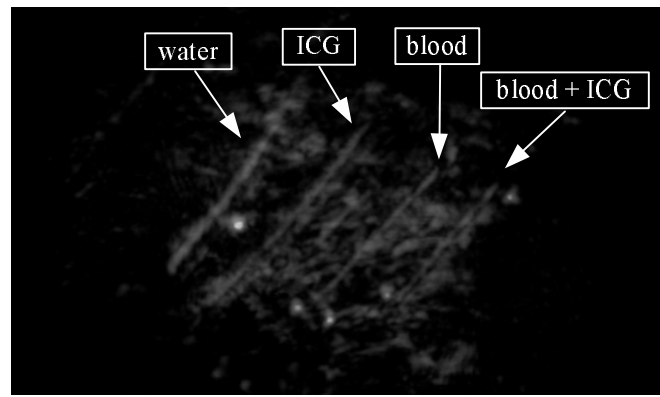
Fig. 6. 3D rendered photoacoustic (red) image overlaid on a pulse-echo image (gray-scale); both reconstructed using the data from a 16 x 16 aperture.

ACKNOWLEDGMENT

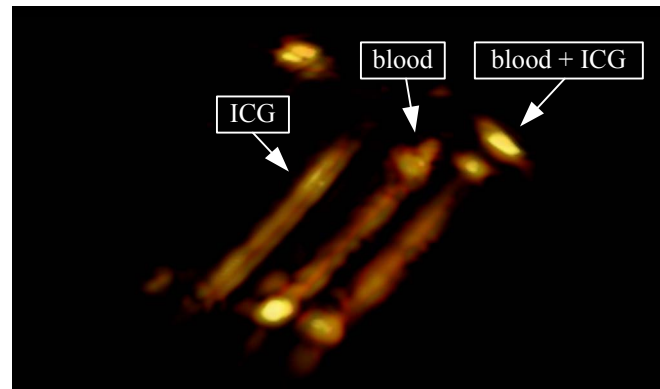
This work was supported by funds from Canon Inc. The authors would like to thank National Semiconductor for the fabrication of the integrated circuits. Larry Randall provided valuable support for machining the experimental equipment. Srikant Vaithilingam was supported by a P. Michael Farmwald Stanford Graduate Fellowship. Xuefeng Zhuang was supported by a Weiland Family Stanford Graduate Fellowship.

REFERENCES

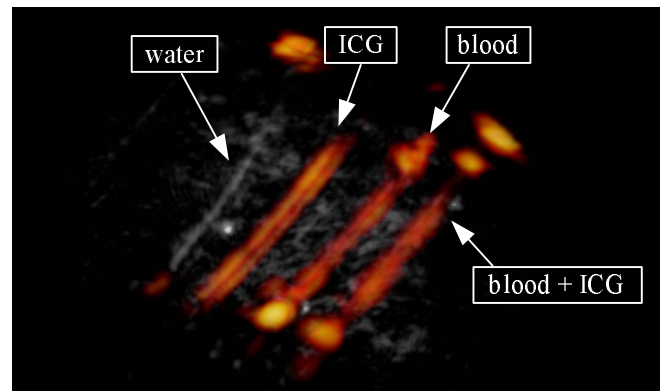
- [1] L. Wang, "Ultrasound-mediated biophotonic imaging: a review of acousto-optical tomography and photo-acoustic tomography," *Journal of Disease Markers*, vol. 19, pp. 123–138, 2004.
- [2] S. Vaithilingam, I. O. Wygant, S. Sifferman, X. Zhuang, Y. Furukawa, Ö. Oralkan, S. Keren, S. S. Gambhir, and B. T. Khuri-Yakub, "Tomographic photoacoustic imaging using capacitive micromachined ultrasonic transducer (CMUT) technology," *IEEE Ultrasonics Symposium, 2006*, pp. 397–400, Oct. 2006.
- [3] A. S. Ergun, Y. Huang, X. Zhuang, Ö. Oralkan, G. G. Yaralioglu, and B. T. Khuri-Yakub, "Capacitive micromachined ultrasonic transducers: Fabrication technology," *IEEE Trans. Ultrason., Ferroelectr., Freq. Control*, vol. 52, no. 12, pp. 2242–2258, 2005.
- [4] X. Jin, I. Ladabaum, and B. T. Khuri-Yakub, "The microfabrication of capacitive ultrasonic transducers," *J. Microelectromech. Syst.*, vol. 7, no. 3, pp. 295–302, Sep 1998.
- [5] I. Wygant, X. Zhuang, D. Yeh, Ö. Oralkan, A. Ergun, M. Karaman, and B. T. Khuri-Yakub, "Integration of 2D CMUT arrays with front-end electronics for volumetric ultrasound imaging," *IEEE Trans. Ultrason., Ferroelectr., Freq. Control*, vol. 55, no. 2, pp. 327–342, February 2008.
- [6] X. Zhuang, A. Nikoozadeh, M. A. Beasley, G. G. Yaralioglu, B. T. Khuri-Yakub, and B. L. Pruitt, "Biocompatible coatings for CMUTs in a harsh, aqueous environment," *Journal of Micromechanics and Microengineering*, vol. 17, no. 5, pp. 994–1001, 2007.
- [7] A. Nikoozadeh, I. Wygant, D.-S. Lin, Ö. Oralkan, A. Ergun, K. Thomeinius, A. Dentinger, D. Wildes, G. Akopyan, K. Shivkumar, A. Mahajan, D. Stephens, D. Sahn, and P. Khuri-Yakub, "Fully integrated CMUT-based forward-looking intracardiac imaging for electrophysiology," *IEEE Ultrasonics Symposium, 2007*, pp. 900–903, Oct. 2007.
- [8] C. Haritoglou, W. Freyer, S. G. Priglinger, and A. Kampik, "Light absorbing properties of indocyanine green (ICG) in solution and after adsorption to the retinal surface – an ex-vivo approach," *Graefe's Archive for Clinical and Experimental Ophthalmology*, vol. 244, pp. 1196–1202, Sep. 2006.
- [9] K. Hollman, K. Rigby, and M. O'Donnell, "Coherence factor of speckle from a multi-row probe," *IEEE Ultrasonics Symposium, 1999*, vol. 2, pp. 1257–1260, 1999.
- [10] P.-C. Li and M.-L. Li, "Adaptive imaging using the generalized coherence factor," *IEEE Trans. Ultrason., Ferroelectr., Freq. Control*, vol. 50, no. 2, pp. 128–141, Feb. 2003.



(a)



(b)



(c)

Fig. 7. Images of chicken breast phantom: (a) 3D rendered pulse-echo image (b) 3D rendered photoacoustic image (c) 3D rendered photoacoustic (red) image overlaid on pulse-echo image (gray-scale).

- [11] C.-K. Liao, M.-L. Li, and P.-C. Li, "Optoacoustic imaging with synthetic aperture focusing and coherence weighting," *Opt. Lett.*, vol. 29, no. 21, pp. 2506–2508, 2004.
- [12] O. Faha, "Osirix: An open source platform for advanced multimodality medical imaging," *4th International Conference on Information & Communications Technology*, pp. 1–2, Dec. 2006.